PROCEEDINGS OF SPIE

Infrared Technology and Applications XXXV

Bjørn F. Andresen
Gabor F. Fulop
Paul R. Norton
Editors

13–17 April 2009
Orlando, Florida, United States

Sponsored and Published by
SPIE

Part One of Two Parts

Volume 7298

Proceedings of SPIE, 0277-786X, v. 7298

Please use the following format to cite material from this book:
Author(s), "Title of Paper," in *Infrared Technology and Applications XXXV*, edited by Bjørn F. Andresen, Gabor F. Fulop, Paul R. Norton, Proceedings of SPIE Vol. 7298 (SPIE, Bellingham, WA, 2009) Article CID Number.

ISSN 0277-786X
ISBN 9780819475640

Published by
SPIE
P.O. Box 10, Bellingham, Washington 98227-0010 USA
Telephone +1 360 676 3290 (Pacific Time) · Fax +1 360 647 1445
SPIE.org

Printed in the United States of America.

Publication of record for individual papers is online in the SPIE Digital Library.

SPIEDigitalLibrary.org

Paper Numbering: Proceedings of SPIE follow an e-First publication model, with papers published first online and then in print and on CD-ROM. Papers are published as they are submitted and meet publication criteria. A unique, consistent, permanent citation identifier (CID) number is assigned to each article at the time of the first publication. Utilization of CIDs allows articles to be fully citable as soon they are published online, and connects the same identifier to all online, print, and electronic versions of the publication. SPIE uses a six-digit CID article numbering system in which:

- The first four digits correspond to the SPIE volume number.
- The last two digits indicate publication order within the volume using a Base 36 numbering system employing both numerals and letters. These two-number sets start with 00, 01, 02, 03, 04, 05, 06, 07, 08, 09, 0A, 0B … 0Z, followed by 10-1Z, 20-2Z, etc.

The CID number appears on each page of the manuscript. The complete citation is used on the first page, and an abbreviated version on subsequent pages. Numbers in the index correspond to the last two digits of the six-digit CID number.

Contents

Part One

IR OPTICS

CRYOCOOLERS FOR IR FOCAL PLANE ARRAYS

TYPE II SUPERLATTICE FPAS

UNCOOLED FPAS AND APPLICATIONS II

SELECTED TECHNOLOGY PRESENTATIONS

SELECTED APPLICATION PRESENTATIONS

Conference Committee

Symposium Chairs

Ray O. Johnson, Lockheed Martin Corp. (United States)
Michael T. Eismann, Air Force Research Laboratory (United States)

Conference Chairs

Bjørn F. Andresen, Elbit Systems Electro-Optics ElOp Ltd. (Israel)
Gabor F. Fulop, Maxtech International, Inc. (United States)
Paul R. Norton, U.S. Army Night Vision & Electronic Sensors Directorate (United States)

Program Committee

Christopher C. Alexay, StingRay Optics, LLC (United States)
Stefan T. Baur, Raytheon Vision Systems (United States)
Philippe François Bois, Thales Research & Technology (France)
Wolfgang A. Cabanski, AIM Infrarot-Module GmbH (Germany)
John T. Caulfield, Cyan Systems (United States)
Peter N. Dennis, QinetiQ Ltd. (United Kingdom)
John W. Devitt, L-3 Communications Cincinnati Electronics, Inc. (United States)
Michael T. Eismann, Air Force Research Laboratory (United States)
Martin H. Ettenberg, Sensors Unlimited, Inc., part of Goodrich Corporation (United States)
Sarath D. Gunapala, Jet Propulsion Laboratory (United States)
Charles M. Hanson, L-3 Communications Infrared Products (United States)
Stuart B. Horn, Defense Advanced Research Projects Agency (United States)
Masafumi Kimata, Ritsumeikan University (Japan)
Hee Chul Lee, Korea Advanced Institute of Science and Technology (South Korea)
Paul D. LeVan, Air Force Research Laboratory (United States)
Wei Lu, Shanghai Institute of Technical Physics (China)
Whitney Mason, U.S. Army Night Vision & Electronic Sensors Directorate (United States)
Mark A. Massie, Nova Sensors (United States)
Paul L. McCarley, Air Force Research Laboratory (United States)
R. Kennedy McEwen, SELEX Sensory and Airborne Systems, Ltd. (United Kingdom)
John Lester Miller, FLIR Systems, Inc. (United States)

A. Fenner Milton, United States Army Night Vision & Electronic Sensors Directorate (United States)
Ofer Nesher, SCD - Semi Conductor Devices (Israel)
Peter W. Norton, BAE Systems, Inc. (United States)
Joseph G. Pellegrino, U.S. Army Night Vision & Electronic Sensors Directorate (United States)
Herbert K. Pollehn, Army Research Laboratory (United States)
Manijeh Razeghi, Northwestern University (United States)
Ingmar G. Renhorn, Swedish Defence Research Agency (Sweden)
Antoni Rogalski, Wojskowa Akademia Techniczna (Poland)
Ingo Rühlich, AIM Infrarot-Module GmbH (Germany)
Myron J. Scholten, DRS Sensors and Targeting Systems, Inc. (United States)
Venkataraman S. Swaminathan, U.S. Army Night Vision & Electronic Sensors Directorate (United States)
Simon Thibault, ImmerVision (Canada)
Meimei Z. Tidrow, Missile Defense Agency (United States)
Jean-Luc Tissot, ULIS (France)
Philippe M. Tribolet, Sofradir (France)
Jay Vizgaitis, U.S. Army Night Vision & Electronic Sensors Directorate (United States)
Kadri Vural, Teledyne Imaging Sensors (United States)

Session Chairs

Infrared at Jet Propulsion Laboratory
Sarath D. Gunapala, Jet Propulsion Laboratory (United States)

CQWIP, QDWELL, and QWIP FPAs
Philippe François Bois, Alcatel-Thales III-V Laboratory (France)
John W. Devitt, L-3 Communications Cincinnati Electronics (United States)

QWIP and QDIP with Antimonides
Philippe F. Bois, Alcatel-Thales III-V Laboratory (France)
John W. Devitt, L-3 Communications Cincinnati Electronics (United States)

Novel Uncooled Technologies
Whitney Mason, U.S. Army Night Vision & Electronic Sensors Directorate (United States)
Joseph G. Pellegrino, U.S. Army Night Vision and Electronic Sensors Directorate (United States)

Uncooled FPAs and Applications I
Stefan T. Baur, Raytheon Vision Systems (United States)
Jean-Luc Tissot, ULIS (France)

IR Optics
Christopher C. Alexay, StingRay Optics, LLC (United States)
Jay N. Vizgaitis, U.S. Army Night Vision and Electronic Sensors Directorate (United States)

Cryocoolers for IR Focal Plane Arrays
Ingo Rühlich, AIM Infrarot-Module GmbH (Germany)
Alexander M. Veprik, RICOR-Cryogenic & Vacuum Systems (Israel)

Infrared in Future Soldier Systems I
Gabor F. Fulop, Maxtech International, Inc. (United States)

Infrared in Future Soldier Systems II
Gabor F. Fulop, Maxtech International, Inc. (United States)

Target Warning Systems
Michael T. Eismann, Air Force Research Laboratory (United States)
Ingmar G. Renhorn, Swedish Defence Research Agency (Sweden)
Gil A. Tidhar, Optigo Systems, Ltd. (Israel)

Type II Superlattice FPAs
Manijeh Razeghi, Northwestern University (United States)
Meimei Z. Tidrow, U.S. Army Night Vision and Electronic Sensors Directorate (United States)

MCT Advanced Research I
Wei Lu, Shanghai Institute of Technical Physics (China)
Joseph G. Pellegrino, U.S. Army Night Vision & Electronic Sensors Directorate (United States)

MCT Advanced Research II
Hee Chul Lee, Korea Advanced Institute of Science and Technology (Korea, Republic of)
Paul D. LeVan, Air Force Research Laboratory (United States)
Joseph G. Pellegrino, U.S. Army Night Vision & Electronic Sensors Directorate (United States)

MCT Advanced Research III
Antoni Rogalski, Wojskowa Akademia Techniczna (Poland)
Gérard L. Destéfanis, CEA-LETI (France)

Uncooled FPAs and Applications II
Masafumi Kimata, Ritsumeikan University (Japan)
Charles M. Hanson, L-3 Communications Infrared Products (United States)

IR Optics: Filters
Jay N. Vizgaitis, U.S. Army Night Vision & Electronic Sensors Directorate (United States)
Christopher C. Alexay, StingRay Optics, LLC (United States)

MCT 50th Anniversary I
Wolfgang A. Cabanski, AIM Infrarot-Module GmbH (Germany)
R. Kennedy McEwen, SELEX GALILEO (United Kingdom)
Philippe M. Tribolet, SOFRADIR (France)
Paul R. Norton, U.S. Army Night Vision & Electronic Sensors Directorate (United States)

MCT 50th Anniversary II
Stefan T. Baur, Raytheon Vision Systems (United States)
Myron J. Scholten, DRS Sensors & Targeting Systems, Inc. (United States)
Kadri Vural, Teledyne Imaging Sensors (United States)
Paul R. Norton, U.S. Army Night Vision & Electronic Sensors Directorate (United States)

MCT 50th Anniversary III
Peter N. Dennis, QinetiQ Ltd. (United Kingdom)
Stuart B. Horn, Defense Advanced Research Projects Agency (United States)
Paul R. Norton, U.S. Army Night Vision & Electronic Sensors Directorate (United States)

Short Wave IR and Applications
Martin H. Ettenberg, Goodrich SUI, Inc. (United States)

Selected Technology Presentations
John L. Miller, FLIR Systems, Inc. (United States)
Simon Thibault, ImmerVision (Canada)
Bjørn F. Andresen, Elbit Systems Electro-Optics ElOp Ltd. (Israel)

Selected Application Presentations
Simon Thibault, ImmerVision (Canada)
John L. Miller, FLIR Systems, Inc. (United States)
Bjørn F. Andresen, Elbit Systems Electro-Optics ElOp Ltd. (Israel)

Introduction

The Thirty-Fifth conference on Infrared Technology and Applications was held the week of April 13-17, 2009 at the Orlando World Center Marriott Resort and Convention Center in Orlando, Florida. The agenda was divided into 22 sessions:

1. Infrared at Jet Propulsion Laboratory
2. CQWIP, QDWELL, and QWIP FPAs
3. QWIP and QDIP with Antimonides
4. Novel Uncooled Technologies
5. Uncooled FPAs and Applications I
6. IR Optics
7. Cryocoolers for IR Focal Plane Arrays
8. Infrared in Future Soldier Systems I
9. Infrared in Future Soldier Systems II
10. Target Warning Systems
11. Type II Superlattice FPAs
12. MCT Advanced Research I
13. MCT Advanced Research II
14. MCT Advanced Research III
15. Uncooled FPAs and Applications II
16. IR Optics: Filters
17. MCT 50th Anniversary I
18. MCT 50th Anniversary II
19. MCT 50th Anniversary III
20. Short Wave IR and Applications
21. Selected Technology Presentations
22. Selected Application Presentations

In addition, there were fifteen poster papers presented for discussion on Thursday evening. Highlights of each session are noted below. Papers cited are referenced as "*-xx*" where the numbers refer to the paper number in the Proceedings, for example *7298-xx*.

1. Infrared at Jet Propulsion Laboratory

This session describes the missions and technologies at the Jet Propulsion Laboratory that relate to the infrared spectrum.

The session was kicked-off with paper -01 (presentation only) giving an overview of JPL's work on infrared space exploration sensors and instruments.

The second paper in the JPL session, -158, describes the development of an LWIR f/1.6 Dyson spectrometer being developed for use in airborne science applications using a QWIP detector array.

Fig. 1 A compact Dyson spectrometer from JPL paper -03.

Compact concentric spectrometers spanning the visible to infrared region (~14 µm) with apertures as low as f/1.4 are discussed in paper -03 from JPL.

Paper -04 presents the results of work on the 6.1 Å lattice antimonide detector materials—InAs, GaSb, and AlSb—by JPL and Raytheon. Imaging of an MWIR Type II material from this effort is shown in a 1024^2 format—see Fig. 2. MWIR bulk antimonides are being made with nBn InAsSb-AlAsSb-GaSb device structures in 640×512 formats with 19 µm pixels. Type II GaInSb-InAs superlattices are used for both MWIR and LWIR spectral regions.

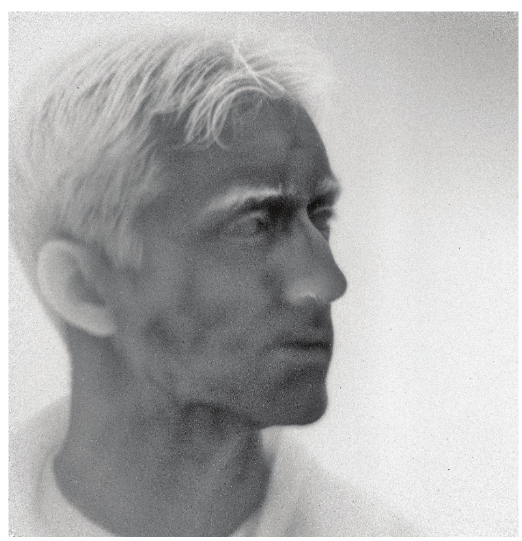

Fig. 2 MWIR InGaSb-InAs Type II MWIR superlattice FPA image in a 1024^2 format having 19 µm pixels from the JPL/Raytheon paper -04.

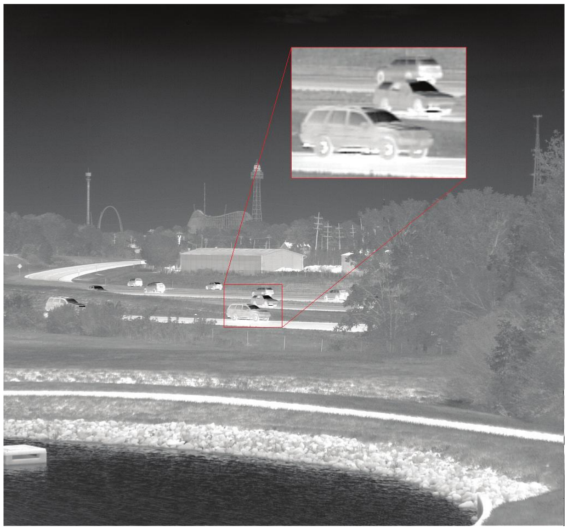

Fig. 3 Corrugated QWIP imagery from a 1024 × 1024 format array described in paper -07.

Novel quantum well intra-subband, sub-monolayer quantum dot, and superlattice devices is the subject of JPL's paper -05. Some consideration is given to the far infrared region, sub-monolayer dots, and the effects of unipolar detector barriers in superlattice structures.

The concluding paper -06 from the JPL session describes large format (640 × 480 and megapixel) multicolor QWIP detectors.

2. CQWIP, QDWELL, and QWIP FPAs

Papers in this session describe variations in the design of quantum well (QWIP) and quantum dot devices (QDOT).

Corrugated quantum well (CQWIP) detector technology and status is reported in paper -07 from the Army Research Laboratory, L-3 Cincinnati Electronics, and Intelligent Epitaxy. Four designs are compared, with collection efficiency in the range from 2.2 to 3.9 %. Imaging with a megapixel array is illustrated with 20 mK NEΔT and 2 msec integration time as shown in Fig. 3.

The University of New Mexico, Caltech, and Tufts University report on multispectral, polarization-sensitve detection using plasmon-assisted cavities and quantum dots-in-a-well detectors (DWELL) in paper -08.

Paper -09 from the University of Massachusetts Lowell concerns smart focal plane arrays combining voltage-tunable quantum dot detectors and flexible electronics printed using a solution of carbon nanotubes.

Field trials of a 640 × 512 dithered QWIP polarization-sensitive camera with 20 μm pixels are described in paper -10 from Thales. Polarization is accomplished with the usual quadrant subarray of grating orientations.

3. QWIP and QDIP with Antimonides

This session continues the quantum well and quantum dot detector topic, adding antimonide materials to the mix.

Use of the "Transfer Matrix Method" to design QWIP detectors is described in paper -11 from the Instituto Tecnologico de Aeronautica and the Naval Postgraduate School. The method gives good agreement with measurements.

Paper -12 from the University of Massachusetts Lowell concerns very long wavelength quantum dot detectors with a 15. 3 μm cutoff. High gain >1000 is reported.

The Japan Ministry of Defense and Fujitsu in paper -13 report on a 40 μm pixel 256 × 256 LWIR (10.3 μm) quantum dot detector using a direct injection readout. An NEΔT of 87 mK was reported at 80 K with f/2.5 optics and 8 msec integration time. The integrated detector dewar assembly with the QDIP array is shown in Fig. 4.

Development of smaller-pixel QWIP detectors is presented in paper -14 from IRnova/Acreo and colleagues at KTH. They note that QWIP quantum efficiency suffers as pixel size is reduced due to reduced grating efficiency. Future development work will explore QDOTs and SLS devices.

Alcatel-Thales III-V Lab describe QWIP array performance spanning the MWIR to VLWIR spectrum in pa-

Fig. 4 Integrated 256 × 256 LWIR QDIP detector-cooler assembly described in paper -13.

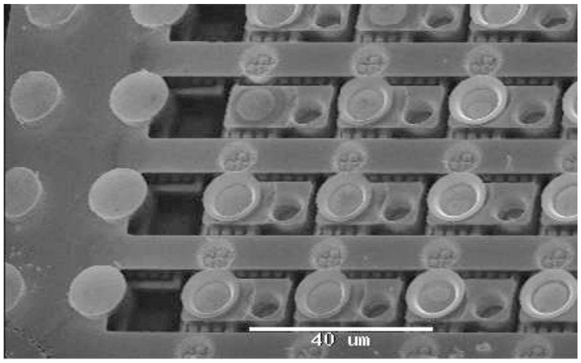

Fig. 5 Dual band QWIP array details. The pixels are on a 25 µm pitch—from paper -15.

per -15. MWIR performance is summarized and also the LWIR production experience for Catherine cameras. Dual-band MWIR/LWIR development progress is underway—array details are shown in Fig. 5.

Paper -16 from SCD presents their progress in the development of antimonide detectors. These include epitaxially-grown InSb, MWIR Type II SLS detectors, and *nBn* devices. Generation-recombination (GR) currents are modeled for 4.6 µm cutoff Type II samples. An *nBn* structure with a 4.0 µm cutoff is reported using InGaSb with an AlGaSb barrier in the conduction band to suppress GR currents.

4. Novel Uncooled Technologies

A variety of novel uncooled technologies were presented, some for the first time. Two papers describe uncooled microcantilever arrays that are read out optically.

Researchers from Koç University in Turkey in paper -17 describe a proposed microcantilever array fabricated from parylene and using an integrated diffraction grating for the optical readout. Current NEΔT is 1 K without optimization but calculations indicate that 10 mK may be possible, theoretically.

In paper -18 Agiltron describes its "Gen III" sensor which it claims has an NEΔT of 92 mK @f/1, but for which no operability could be provided.

Sirica describes progress on its uncooled photon detector that makes use of up-conversion from LWIR to NIR in paper -19. The company relies on the absorption of infrared radiation by free carriers in crystalline silicon clusters of mesoscopic size, followed by the emission of NIR. The company hopes to have a prototype by the end of the year.

Researchers from the University of Missouri describe in paper -20 the characterization of SiGeO films that may hold out higher temperature coefficient of resistance (TCR) for microbolometers although the experiments showed that these films are beset with highly erratic behavior as a function of temperature.

The use of cross-patterned resistive sheets as wavelength selective elements for detectors is described in paper 21 by the University of Texas at Austin.

In paper -22 Delphi and Symetrix propose an active mode ferroelectric array based on strontium bismuth tantalate. The active mode operation eliminates the need for a chopper and has the potential for a higher effective pyroelectric coefficient. Tests on a single element device are presented.

Ann Arbor Sensor Systems in paper -23 outlines the design of their new ultra-low-cost 80 × 60 thermopile array. The device details are shown in Fig. 6. The projected NEΔT of this array is 100 mK @30 Hz, and f/0.8.

Korea Advanced Institute of Science and Technology, KAIST, considers in paper -142 the feasibility of using thin nickel oxide film as a microbolometer material. The developed material is CMOS-compatible, showed a TCR value of -3.28 % and a noise characteristic comparable to that of amorphous silicon. Fig 7 shows the temperature dependence of resistance. The authors therefore consider thin nickel oxide film as being suitable for use as a micro-bolometric material.

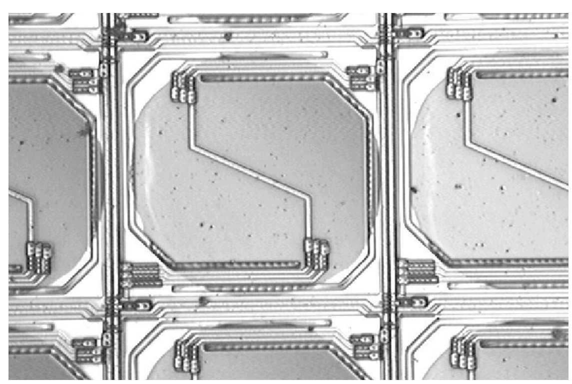

Fig. 6 Details of an 80 × 60 uncooled thermopile array from paper -23.

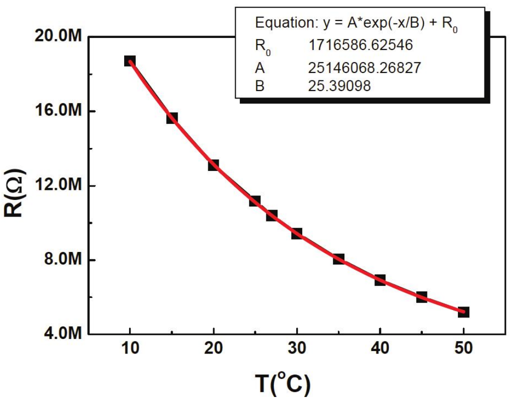

Fig. 7 Temperature dependence of a nickel-oxide film with a TCR of 3.3 % at 27 °C from paper -142.

5. Uncooled FPAs and Applications I

The development of 17 µm pixel technology is described in papers -24 and -27 by VO_x microbolometer manufacturers BAE Systems and DRS with the achievement of NEΔT < 50 mK in 640 × 480 arrays and development of 1024 × 768 array in progress. FPA pixel-size implications are illustrated in Fig. 8.

Ulis describes its 1024 × 768 a-Si microbolometers with 17 µm pixels that has attained an NEΔT of 47 mK (with a dynamic range of 170 °C) and is very stable from 0 to 60 °C without a TEC cooler—see paper -25.

In paper -26 SCD outlines the development of its 640 × 480 17 µm VO_x microbolometer which it projects will achieve an NEΔT of 50 mK.

In amorphous silicon technology, L-3 Infrared Products outlines in paper -28 its development of 320 × 240, 640 × 480 and 1024 × 768 microbolometers with 17 µm pixels. The company is concentrating on an alloy of amorphous silicon with a higher TCR that does not have higher 1/f noise.

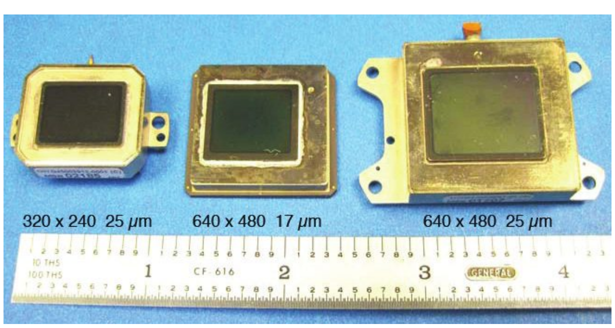

Fig. 8 Comparison of VOx microbolometer packages from paper -27.

Elbit ElOp in paper -156 summarizes the applications of uncooled technology to soldier sights.

There were two papers on uncooled SOI (silicon-on-insulator) technology that makes use of the temperature change in single crystal pn junctions exposed to infrared radiation:

In paper -31 Mitsubishi Electric describes a novel ROIC for TEC-less operation of SOI FPAs based on thermally isolated reference pixels. The method eliminates the need for extensive non-uniformity correction (NUC) tables.

Toshiba summarizes the development of a low-cost 160 × 120 SOI FPA which is operated without temperature stabilization—see paper -32. Current NEΔTs are approximately 500 mK but have not been optimized.

Electro-optic Sensor Design in paper -33 describes laboratory and field tests of a low-cost microbolometer concept that could replace current PIR security sensors.

6. IR Optics

Target acquisition systems operating in detection mode require a large field of view for situational awareness. Immervision describes in paper -34 the design of a panomorphic LWIR lens with a hemispherical field of view. A region of interest, which includes potential targets, is defined for each specific system application. The optical system provides a higher spatial resolution, meaning a better detection capability, in this region. An IRFPA of relatively modest pixel count may therefore be used for the hemispherical operation.

Qioptiq reviews in paper -35 ways to increase performance and reduce the cost of uncooled system optics while keeping the number of elements at a minimum of two. This is achieved by use of aspheric and diffractive surfaces. Computational imaging techniques are seen as an important future addition to the optical designer's tools. Several design examples are discussed.

NVESD attacks in paper -36 the challenge of designing optics with high simultaneous performance in the SWIR and MWIR bands. The use of this type of optical systems is essential in, among others, next generation thermal imagers which require the ability to detect and identify targets with a single compact imaging system having one IRFPA. Multiple approaches are analyzed including use of alternate materials and design tech-

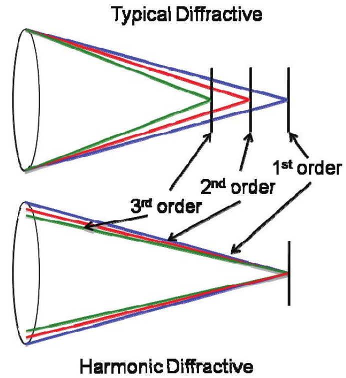

Fig. 9 Paper -36 shows improved color correction with harmonic diffractive design.

niques. Harmonic diffractive lenses, illustrated in Fig. 9, were considered for color correction.

Imaging a bright source against a low-light background can cause image-degrading artifacts and noise in NIR and SWIR cameras—see Fig. 10. StingRay Optics discusses this phenomenon in paper -37. It is caused by reflections and scattering inside the lens housing rather than by optical design. The reduction of this problem by grinding and coating of mechanical and optical surfaces is clearly demonstrated.

Optical Dynamics, in cooperation with University of Kentucky, demonstrates in paper -38 for the first time a polymer / nanoparticle composite thin film suitable for making NIR / SWIR mirrors on plastic and flexible substrates. These films maintain adhesion under high strains while earlier attempts failed due to mismatches in mechanical properties that led to reduction of the interfacial adhesion.

Paper -39 by the Czech Institute of Scientific Instruments, in cooperation with Acktar of Israel, reports on emissivity measurements on various coatings at temperatures between 10 K and 300 K. The measurements are primarily of relevance to space and cryogenic applications. While all coatings withstand cryogenic and vacuum conditions, for very thin coatings Acktar's own Fractal Black is found to have the highest emissivity and lowest outgassing. That coating also produces the most accurate coating geometry for optical parts.

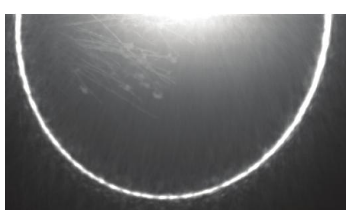

Fig. 10 Ring image artifact discussed in paper -37

7. Cryocoolers for IR Focal Plane Arrays

Air Liquide presents in paper -40 two Pulse Tube Coolers (PTC) – one miniature and one large – for use on earth observation missions. The former is designed for cooling detectors to 80 K while the larger one cools the detectors to temperatures below 50 K. Details of their Cooler Drive Electronics are given.

New Cooler Drive Electronics for Stirling and Pulse Tube cryogenic coolers are described by Thales Cryogenics in paper -42. Significant progress is reported in terms of accuracy, stability and size of these components which measure and control the temperature for several of the company's flexure bearing coolers. In response to performance requirements for 3rd generation FPAs, a trend is identified towards cooling to temperatures higher than the conventional 77 K, leading to significantly lower cooler size, weight and power.

Sensor systems required to operate at temperatures higher than 77 K have spurred developments of new FPAs and cryogenic coolers optimized for these temperatures. The drivers behind these developments are the need for smaller and more reliable systems with longer life, demand for less power and shorter cool-down times. Ricor reports in paper -43 on a novel microminiature split Stirling linear cryocooler design having a shortened cold finger which makes it attractive for TWS and UAV-mounted systems at higher temperature.

100 % testing of cryocoolers at the manufacturing stage is a time-consuming process. Thales Cryogenie of France reports in paper -44 on their use of the Six Sigma method to effectively lower the manufacturing defect rate. Their success has enabled the use of sample testing on the manufacturing line of a rotary Stirling cooler. The new test procedure is validated by the 0.5% reject rate found after 100% post integration performance testing at the customer's premises. The root causes of the performance variability is defined and discussed.

Miniature UAVs, small arms sights and tactical night vision goggles require light and small cryocoolers. Ricor, in paper -45, has taken advantage of the recent reduction in dark current of some FPAs to design a microminiature cryocooler operating in the 95K to 110 K range. The size of their small cooler is one third of their standard tactical cryocooler—see Fig. 11.

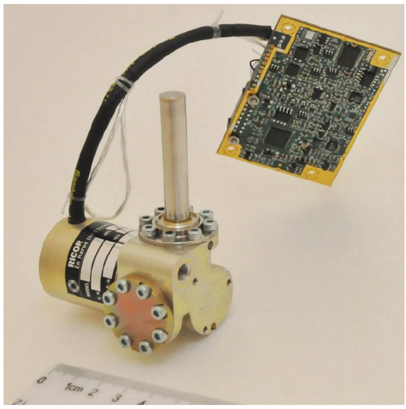

Fig. 11 Microminiature cryocooler with digital controller, from paper -45.

The selection of type and specific characteristics of infrared detector cryocoolers is driven by the intended system application and cost considerations. AIM Infrarot-Module reviews in paper -46 how updated system performance requirements have led to new development trends for the coolers. MTTF is used as the measure for reliability. A near 6-year MTTF is reported for AIM's new, small cooler which employs a Pulse-Tube coldfinger.

Following a thorough feasibility study, the researchers from Soreq NRC and Ricor, paper -47, built and tested a new concept for the driver of the linear compressor of a micro miniature split Stirling cryogenic cooler. The proposed "pumping driver" is current ripple - free and therefore lends itself towards a compact design without the need for oversized battery packs and power electronic components.

The cryocooler is often the critical subsystem which determines the operating time before breakdown of an infrared sensor system. Carleton Life Support Systems reports in paper -147 on the operating time of their OWL cryogenic cooler which is required to have a mean time to failure, MTTF, of 12,000 hours. In test the coolers are found to operate 25% longer than the required MTTF.

8 and 9. Infrared in Future Soldier Systems

In the introduction to this session, a distinction was made between the various infrared sights and cameras used in soldier systems versus the formal Future Soldier programs that numerous countries are developing. The formal programs include a comprehensive approach in which infrared is only one part. Typically such formal programs include—in addition to sensors—soldier protective equipment, a helmet with HUD, a personal computer, and a way to share images and data over a network.

In this session, presentations on both formal Future Soldier Systems and various potential infrared sensors are presented.

Since the U.S. program is in transition, no presentations from the Land Warrior or the new Ground Soldier System (GSS) - or its first increment the Ground Soldier Ensemble (GSE) – were available. In the U.S., the development and fielding of sensor systems has outrun the formal programs especially in the Thermal Weapon Sight (TWS) program.

Therefore, in this session, the two presentations from the U.S. concentrate on potential future infrared sensors—rather than on the formal programs.

L-3 Electro-Optical Systems in paper -48 outlines progress made in digital image fusion between an image intensifier coupled to a CMOS imager and an uncooled microbolometer. Major improvements of range performance were claimed for a wide field-of-view prototype digital enhanced night vision goggle (ENVG).

In paper -49 Fairchild Imaging describes a low-light level CMOS imager which is well suited for digitally fused night vision systems. Although the CMOS imager is not as sensitive as a GEN III image intensifier tube under overcast starlight, it offers a wider dynamic range, no blooming, higher reliability, smaller size, lower weight, and lower cost.

Sagem presents an overview of the FELIN French future soldier system in paper -50 which includes a binocular based on uncooled microbolometers and thermal weapon sights for the infantryman and snipers—see Fig. 12. The system also includes image capture and dissemination.

Two presentations were made on the German IdZ-ES infantryman of the future program.

Jena Optronik GmbH describes the Handheld Multifunctional Thermal Imager, which includes both visible and thermal (384×288 HgCdTe MWIR FPA) channels, together with a laser rangefinder (LRF), digital magnetic Compass (DMC) and GPS in paper -51.

Fig. 12 French FELIN system architecture from paper -50

Carl Zeiss Optronics GmbH presents in paper -52 the IdZ-ES Small Arms Video Sight which includes both visible and thermal (384 × 288 uncooled microbolometer) channels, together with a laser rangefinder (LRF), Digital Magnetic Compass (DMC) and GPS.

In paper -53 the Defence Research and Development Canada outlines the Canadian Integrated Soldier System Project (ISSP). Currently several Technology Demonstration programs are underway, including studies of night vision goggles and fused I2/IR systems for head-mounted use.

Optigo Systems (Israel) describes a gunshot detection system for protecting soldiers in paper -54. The system makes use of a SWIR detector

10. Target Warning Systems

Night and day situational awareness for mounted soldiers in stationary and moving ground vehicles is the subject discussed by FLIR Systems in paper -55. By use of electronic stitching three images are combined to give a full 180 degrees FOV. The imager, using a 640 × 480 pixel uncooled microbolometer, achieves recognition of a man sized target at 200 meter range under good visibility conditions, as shown in Fig. 13. The image processing, including stitching, distortion correction and scene-based non-uniformity correction is discussed in some detail.

BAE Systems presents in paper -56 results of a study on the optimum types and combinations of sensors needed for giving the mounted warfighter a 360 degree situational awareness under "closed-hatch" conditions. Both theoretical and on-vehicle investigations are performed. While the uncooled LWIR sensor is preferred for detection, the fusion of Visible or NIR with LWIR is found to offer solid user benefit for identification—see Fig. 14.

Elisra discusses in paper -57 aspects of a helicopter mounted passive infrared system, the SAPIR. The system tracks and monitors other helicopters which are

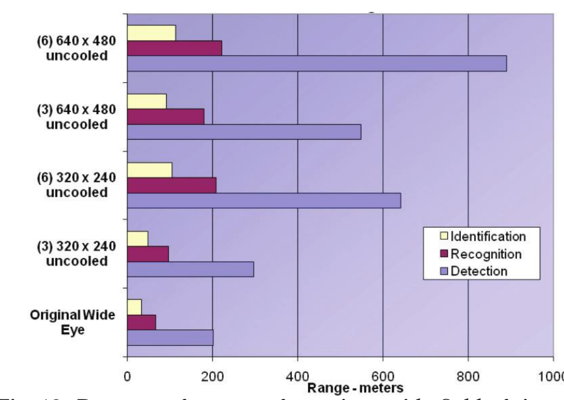

Fig. 13 Range performance for various wide-field-of view concepts discussed in paper -55.

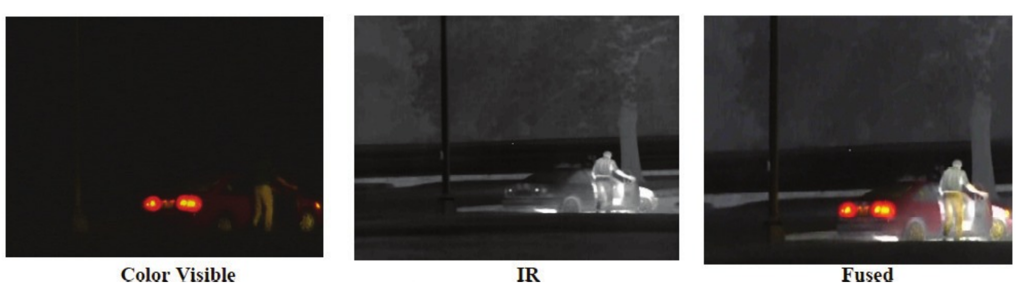

Fig. 14 Fusion of visible and infrared imagery demonstrated in paper -56.

getting too close or are on collision course. SAPIR thus lowers the pilot`s workload while performing operational missions. The collision avoidance system processes the signals obtained from the helicopters missile warning system, the PAWS. The operational problem is discussed in some detail.

Man portable air defense missiles and ground fire represent the greatest threats to aircraft – military as well as civilian. The subject of M&M Aviation's paper -60 is clutter suppression in NIR missile warning systems. The clutter can severely reduce the probability of threat detection. The company discussed their SIMAC algorithm which makes use of multiple spatial and spectral filtering techniques. Test flights have demonstrated up to two orders of magnitude reduction in false alarms/ false tracks for the same probability of point target detection when compared to other processing techniques.

11. Type II Superlattice FPAs

The Type II superlattice session includes papers on the progress towards developing detector and focal plane arrays using this technology in both the MWIR and LWIR spectral bands. Also included is a report from the first Type II superlattice production program.

Progress in superlattice detector development has inspired a new Missile Defense Agency approach for detector production as reported in paper -61 from NVESD, IDA, and MDA. The new approach is a horizontal structure where materials growth, array fabrication, readouts, and FPA assembly are each done by separate organizations rather than by a single organization.

Paper -62 from the University of New Mexico and Korea Research Institute of Standards and Science describe LWIR Type II superlattice detectors using *nBn* and *pin* structures. The *nBn* device is reported to give higher performance.

LWIR (9.6 μm) Type II superlattice detectors that are background limited at 77 K with a 300 K, 2π field of view are reported in paper -63 from Northwestern University. Improvements in quantum efficiency and R_0A using "M" structure barriers are noteworthy.

The German team of Fraunhofer and AIM report on their continuing experience in the production of two-color MW/MW Type II SLS detectors in paper -64. Figure 15 shows an SEM image of 3-bump array pixels.

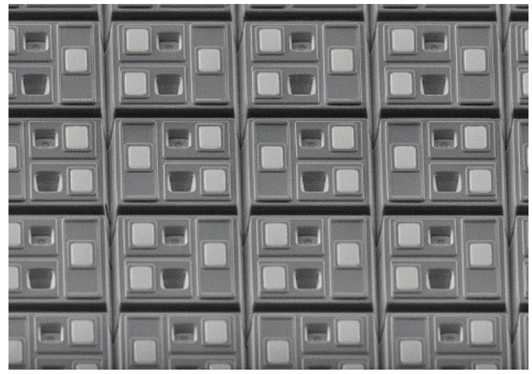

Fig. 15 A portion of the 384 × 288 two-color MW/MW Type II SLS detector array in paper -64.

Paper -65 on the fabrication of LWIR Type II SLS diodes is from HRL. Tellurium ion implantation and Zn diffusion were compared for forming the junction. Zinc-diffused diodes exhibited GR leakage. Work is underway to utilize tellurium diffusion for an n-on-p structure.

Growth of Type II SLS detectors on GaAs rather than GaSb is the subject of paper -66 from Northwestern University. Although GaAs has a 7 % lattice mismatch compared with GaSb, both MWIR and LWIR Type II layers are reported with promising results.

The impact of minority carrier lifetime on the performance of Type II SLS devices is demonstrated in paper -67 from the Night Vision and Electronic Sensors Directorate. Modeling of current-voltage curves shows that current LWIR Type II devices are generation-recombination current-limited with an estimated lifetime of 35 nsec. Lifetime comparisons between Type II SLS detectors and HgCdTe are shown in Fig. 16.

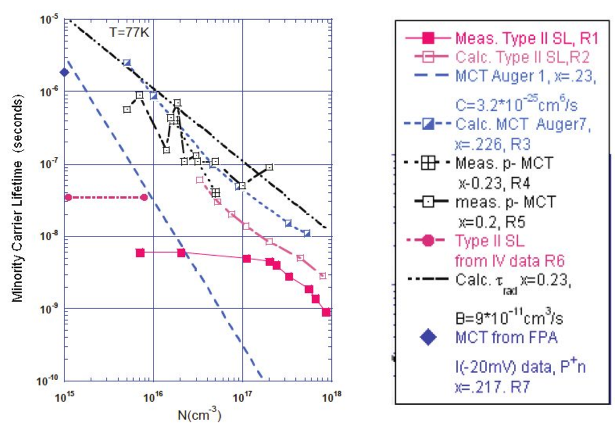

Fig. 16 Measured and calculated minority carrier lifetime for LWIR p- and n-type MCT and p-type LWIR Type II InAs/GaSb superlattice materials. Details are in paper -67.

12, 13, and 14. MCT Advanced Research

The eleven papers in these sessions represent a tribute to the continuing strong importance of HgCdTe detector technology to the infrared community. Note that additional papers on current HgCdTe work are included in Anniversary Sessions 17-19 and in Session 20 on Short Wave IR.

Paper -69 from Sofradir discusses commonalities and differences between HgCdTe detectors used in tactical and space applications. Methods of assessing reliability are reviewed. Examples are given for cooldown cycle reliability.

HgCdTe detector performance spanning the SWIR to VLWIR spectrum are reviewed in paper -70 from AIM. Recent work has reduced pixel pitch to 15 µm with arrays of 640 × 512 format and added short wavelength cutoff devices with 384 × 288 and 1024 × 256 format to expand the range of applications. VLWIR devices are also being developed. Future dual-band HgCdTe devices are to be produced using MBE growth.

DRS reports on the development of a 320 × 6 scanning array in paper -71 that has response from the visible to the SWIR. Spectral response modeling is considered.

Large format, LWIR dual-band detectors are described by RVS in paper -72. Formats of 512 × 512 with 30 µm pixels are fabricated from triple heterojunction layers grown on CdZnTe using a 10-inch MBE system. The spectral response of the array is illustrated in Fig. 17. An NEQ with 98 % operability is reported.

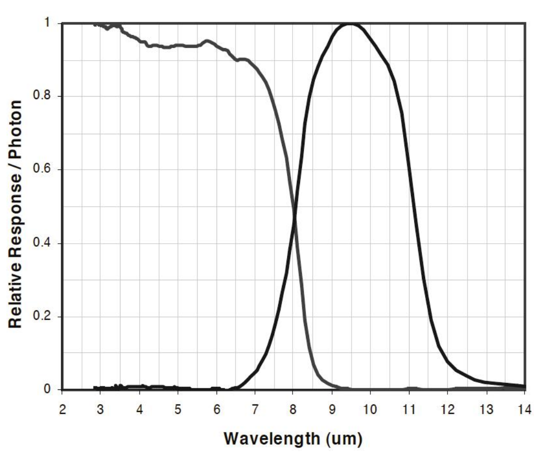

Fig. 17 Dual-band LWIR/LWIR spectral response from and MBE-grown HgCdTe array described in paper -72.

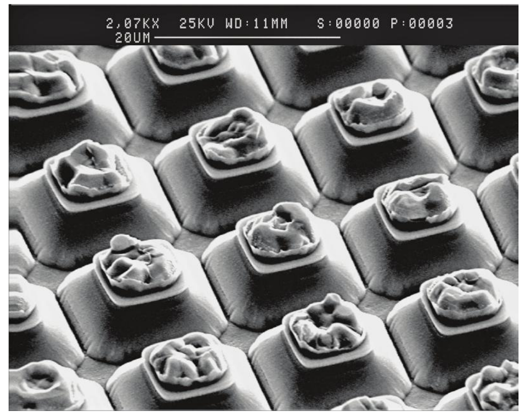

Fig. 18 Dry-etched pixels of MOVPE-grown HgCdTe on GaAs substrates reported in paper -74.

Paper -74 from Selex describes MOVPE-grown HgCdTe on 75 mm GaAs substrates fabricated into 640 × 512 LWIR arrays with 16 µm pixels. The dry-etched mesa pixels are shown in Fig. 18. With a cutoff of 9.4 µm, the array operability is reported to be 99.96 %.

Development of VLWIR HgCdTe arrays at DEFIR using LPE-grown layers on CdZnTe substrates is reported in paper -75. Both p-on-n and n-on-p diode polarities are compared—an example is shown in Fig. 19. At 15 µm the cutoff standard variation is measured to be on the order of 0.1 - 0.2 µm.

Selex describes VLWIR HgCdTe arrays using MOVPE-grown HgCdTe on GaAs in paper -76. BLIP performance is noted at f/5 with a cutoff around 15 µm for temperatures below 70 K.

Paper -77 from DEFIR provides the status of HgCdTe technology on CdZnTe and Ge substrates, including

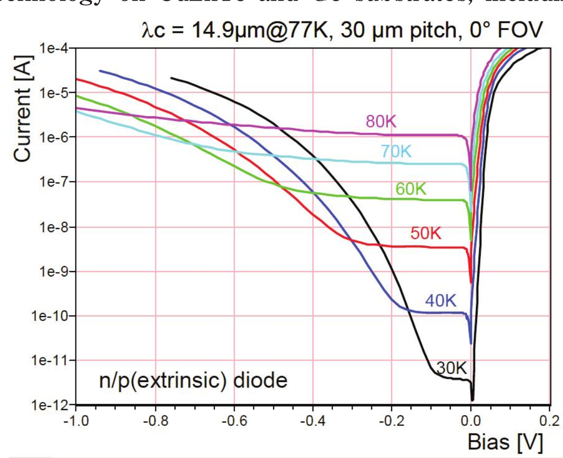

Fig. 19 Diode leakage current for an n-on-p implanted diode described in paper -75.

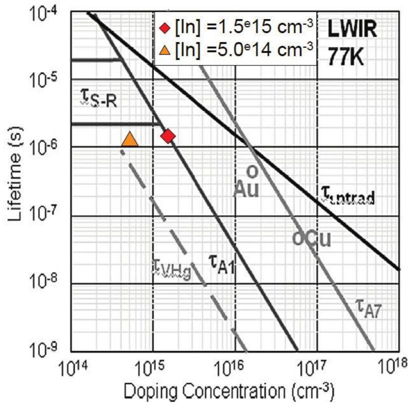

Fig. 20 Minority carrier lifetime exceeds 1 μsec for two indium-doped LWIR samples at 77 K discussed in paper -77.

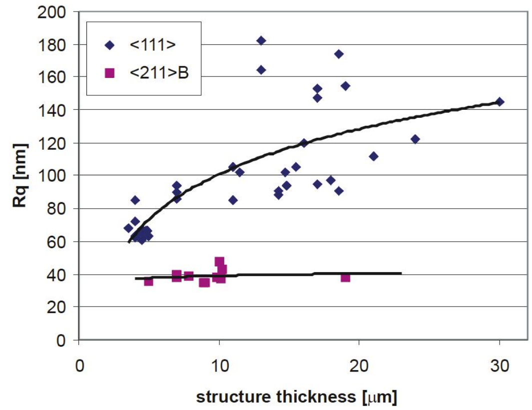

Fig. 22 Minority carrier lifetime exceeds 1 μsec for two indium-doped LWIR samples at 77 K discussed in paper -77.

SWIR and MWIR grown by MBE, and LWIR grown by LPE. Both p-on-n and n-on-p diode polarities are compared. Long carrier lifetime was measured at 77 K in LWIR n-type material as shown in Fig. 20.

TE-cooled HgCdTe detectors with spectral response out to 16 μm is reported in paper -159 from Vigo Systems. These are single-element, optically-immersed detectors using the GaAs substrate as the immersion lens material for the MOCVD-grown hetrojunctions. Fig. 21 shows the device with a 2-stage cooler.

In paper -154 the Military University of Technology in Warsaw, in cooperation with the VIGO System company, report on a study of the surface quality of HgCdTe layers deposited by MOCVD on GaAs substrates. The effect of selected growth parameters on the morphology state is discussed—Fig. 22 shows an example. The importance of GaAs substrate quality and its decisive role for HgCdTe heterostructure morphology smoothness is pointed out.

Fig. 21. Optically-immersed, LWIR HgCdTe detector described in paper -159. The lens is formed from the GaAs detector substrate.

15. Uncooled FPAs and Applications II

In this session a variety of developments in uncooled detector technology were reported.

INO describes in papers -79 and -80 a specially developed space-qualified 512 × 3 VO_x microbolometer and a 640 × 480 microbolometer camera core based on a Ulis amorphous-silicon microbolometer.

Bridge Semiconductor summarizes its development of a thin film ferroelectric FPA which is hybridized to an ROIC in paper -81. Work on a new ROIC is expected to improve performance.

In paper -82 CIDA (Spain) presents progress in its vapor deposited polycrystalline PbSe FPAs. Researchers have demonstrated frame rates as high as 20 kHz on their 16 × 16 FPAs.

Ritsumeikan University (Japan) has developed a low-cost vacuum packaging technology for the mass production of uncooled FPAs as described in paper -83. Also included is a micro-vacuum gauge for monitoring the vacuum inside the FPA vacuum package.

Ulis reports in paper -84 its latest 384 × 288 microbolometer with 25 μm pixels and its adaptability to TEC-less operation which is greatly simplified due to the stability and uniformity of amorphous silicon films. Figure 23 shows an image from the microbolometer.

Samsung Thales demonstrates in paper -135 a method for eliminating image blurring in uncooled FPAs due to the difference in f-number between the FPA and the

Fig. 23 Image from TEC-less 320 × 240 microbolometer presented in paper-84.

optics by using a warm shield between the detector and the lens—see Fig. 24.

Researchers at Dresden University and DIAS describe in paper -141 a new single element pyroelectric detector having a thin (<10 µm) responsive element with high D* and low microphonics.

LIG Nex1 and the Agency for Defence Development (Korea) describe in paper-143 a real-time Non-Uniformity Correction (NUC) scheme for uncooled FPAs implemented in hardware rather than software. The detector is intended for a missile application.

Linkoping University researchers outline in paper -149 the design of a low-noise ROIC for a 64 × 64 uncooled detector array. The ROIC relies on a number of blind and thermally isolated pixels as reference detectors.

Researchers from Middle East Technical University describe in paper -152 a bias heating cancellation method for resistive uncooled microbolometer detectors. The same laboratory discusses in paper -153 a column-based two-stage analog-to-digital converter for uncooled microbolometers.

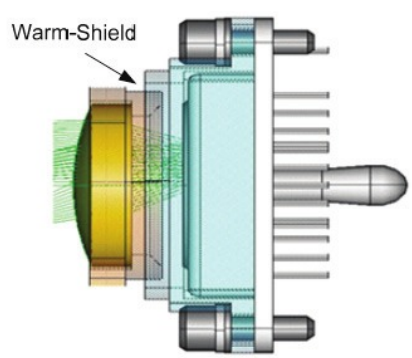

Fig. 24 Detector warm shield described in paper -135

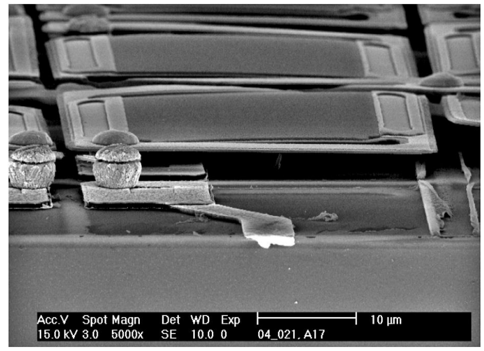

Fig. 25 Uncooled microbolometer pixel from paper -149.

16. IR Optics: Filters

Following detection of a target, its spectral investigation can greatly facilitate its identification. Teledyne Scientific & Imaging reports in paper -85 on their first integrated tunable MEMS Fabry-Perot filter - LWIR FPA which enables spatially resolved spectral tuning in a compact architecture. The ability to tune individual subarrays of pixels to different wavelengths reduces the number of subframes required to investigate a scene and thereby reduces the computational burden of conventional spectral imagers.

Dual band systems require dual band filters. 3rd generation thermal imagers require dual band filters operating in the MW and LW regions. Rugate Technologies reports in paper -87 on their investigation of three types of filters, a Vis – IR beamsplitter, a LW edge filter and a dual bandpass cold filter. Several design techniques are discussed in some depth and the results of an initial set of fabrication runs are presented in order to assess the performance sensitivity to manufacturing errors.

Figure 26 shows an infrared multi-bandpass filter described in paper -88 that blocks wavelengths in the atmospheric absorption bands in order to decrease the

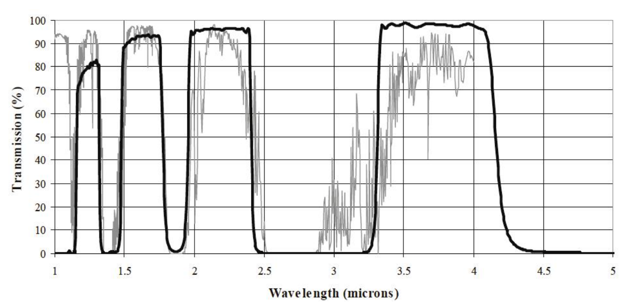

Fig. 26 Transmission of a filter (dark line) designed to transmit the atmospheric windows as described in paper-88.

noise of an infrared system. JDSU shows that their Ucp-1 magnetron sputtering technology has significantly increased the quality of this type of filters relative to filters produced using a thermal evaporation process. To show this, an infrared atmospheric window quadruple bandpass filter is coated and measured. The measured filter transmittance agrees excellently with the theoretical design for both the transmission levels and edge slopes.

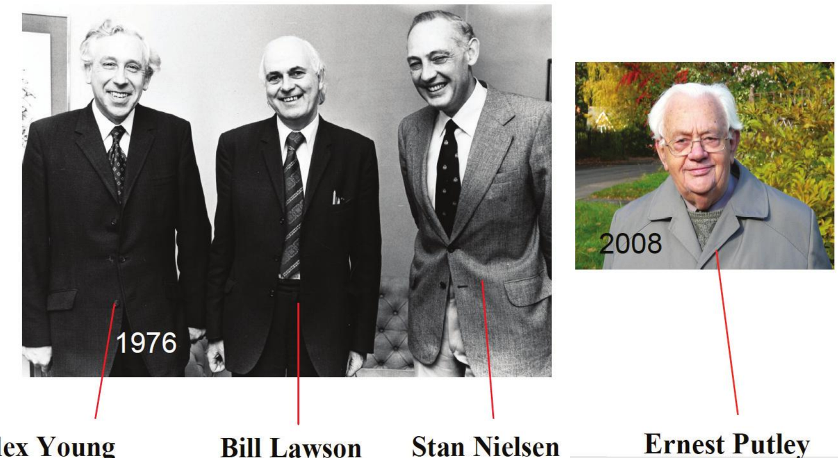

Fig. 27. Pictured are the three Royal Radar Establishment inventors of HgCdTe—Lawson, Nielsen and Young—that disclosed the compound alloy semiconductor material in a 1957 patent. They were joined by Putley in the first publication dated in early 1959 as described in paper -89.

Compactness is an absolute requirement for IR systems designed for the future soldier. Vectronix's paper -155 demonstrates the integration of their SWIR laser range finder into the LWIR optical channel of an uncooled thermal imager. The integration is achieved by development of dual band coatings and use of aspheric and aspherodiffractive lenses made from the GASIR 1 material.

17, 18, and 19 MCT 50th Anniversary

2009 marks the 50th anniversary of the first publication describing the ternary alloy semiconductor HgCdTe by Lawson and colleagues in the UK—see Fig. 27. To celebrate this occasion, a special session was organized to bring together most of the research centers and industrial companies that have participated in the subsequent development of this material into the most versatile and successful infrared detector material in the world today.

Invited papers were solicited from all the laboratories, research centers, and companies known at this time to be involved in HgCdTe technology and development, or that have played a significant role in the past 50 years. All papers in this special session covered the same topics from the special perspective of the individual contributors; namely:

- History and milestones in HgCdTe technologyv development
    - Materials growth
    - Device processing
    - Device design
- Current status of HgCdTe technology

Papers were presented from the following:

United Kingdom	-89	
France	-90	
Germany	-91	
Russia	-92	
Poland	-93	
United States		
Honeywell		-94
BAE Systems		-95
Texas Instruments/DRS		-96
Raytheon Vision Systems		-97
Teledyne		-98
Israel	-99	
Japan	-100	
Korea	-101	
China	-102	
Australia	-103	
India	-104	

A final presentation-only paper from NVESD reviewed contributions to, and support for, HgCdTe science and technology from Universities and Government Laboratories in the United States.

The session concluded with a Government panel that provided observations on the accomplishments of HgCdTe to Defense and Security, as well as the challenges still ahead.

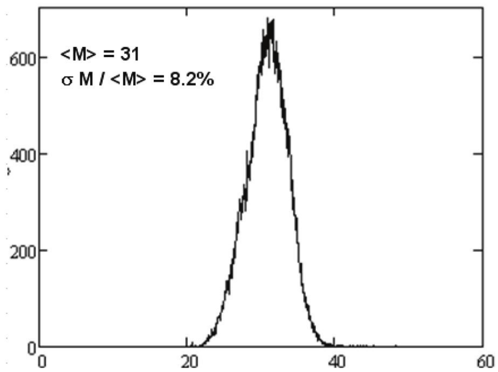

Fig. 28 Histogram of APD gain at 6 V reverse bias as described in paper -106.

20. Short Wave IR and Applications

Interest in the SWIR spectral band has grown considerably in the past few years. This is reflected in the fourteen papers in this session. There are several realms of interest in SWIR, including the potential replacemnt of image intensifiers, 3D ladar imaging, and the combination of passive-active systems.

Paper -105 from the French-German Research Institute and the Technical Center for Weapons and Ammunition discusses 3D range-gated imaging and super-resolution. A laser at 1.5 μm is used together with an electron-bombarded CMOS sensor to image with 9 nsec pulses.

Sofradir and CEA report on MWIR HgCdTe detectors as electron-APDs with an ~1.2 average excess-noise factor for range-gated imaging in paper -106. A new dual-gain CTIA ROIC in a 320 × 256 format with 30 μm pixels is described. Uniformity of APD gain is shown if Fig. 28.

In paper -107 the development of the e-APD detector technology is continued in more detail, with a range of spectral cutoff values and doping methods being characterized. A new detector structure—see Fig. 29—is also reported.

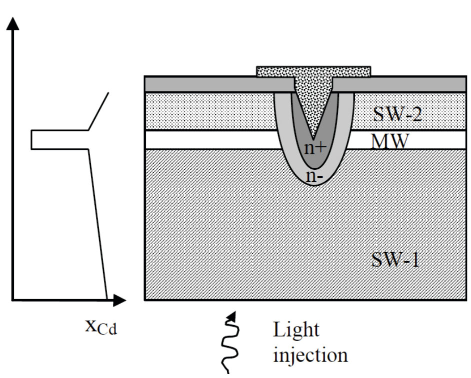

Fig. 29 Horizontal gain well APD structure from paper -107.

Sagem presents a theoretical comparison of SWIR active-imaging detectors in paper -108. InGaAs, HgCdTe, and electron-bombarded InGaAs/InP devices are compared.

Using a InAlAs multiplication layer, APDs are described in paper -109 from the University of Sheffield. Response out to 2.4 μm is reported. Gain at room temperature is 30 and rises to >100 at 200 K.

DRS discusses modeling and performance measurements of cylindrical-geometry HDVIP e-APDs in paper -110. Among parameters assessed are APD fill factor, point spread function, crosstalk, MTF, electron diffusion length, n-region doping concentration, and capacitance vs. bias.

SiGeC CMOS APDs are the subject of paper -111 from Quantum Semiconductor. They are developing a monolithic CMOS array with an epitaxially-grown SiGeC superlattice detector layer that can extend the spectral response into the SWIR spectral region compared to silicon CMOS detectors that are limited to about 1 μm.

The University of Sheffield report on low noise InAs e-APD detectors in paper -112. The noise of InAs APDs is said to be comparable to MWIR HgCdTe e-APDs and requires less cooling—see Fig. 30.

Paper -113 (presentation only) from the Naval Research Laboratory, discussed maritime applications for active infrared imaging.

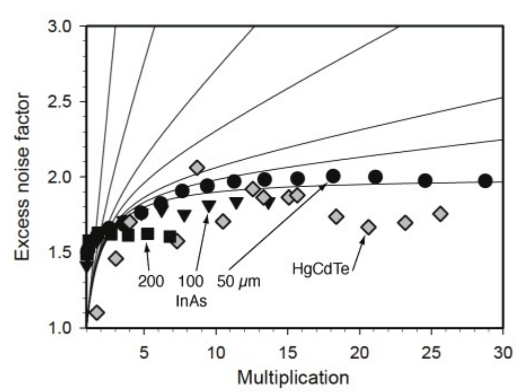

Fig. 30 Excess noise factor for InAs APDs compared with HgCdTe APDs reported in paper -112.

Fig. 31 SWIR image from paper -116 using a MANTIS III camera and local-area contrast to bring out detail from dark areas and suppress saturation in bright areas.

Goodrich, Sensors Unlimited presents work on the development of a large, 1280 × 1024, InGaAs FPA with 15 μm pixels in paper -114. The readout features a CTIA with <50 noise electrons, dual gain, and an on-chip temperature sensor combined with temperature adjusted non-uniformity correction.

In paper -115 SiGe detector arrays are evaluated by Magnolia Optical Technologies and colleagues. Ge diodes grown on silicon are measured with a response in the range of 1.55 - 1.60 μm.

RVS presents results in paper -116 on large format, 1280 × 1024, 15 μm pixel SWIR FPAs with dark current of 1 nA/cm^2, and a noise level of 5 electrons. Novel circuitry provides very high dynamic range—see Fig. 31.

Paper -117 from Aerius Photonics, RVS, and the Santa Barbara Instrument Group reports on low dark current, 0.88 nA/cm^2 at 280 K, InGaAs detectors for night vision and astronomy. Results for astronomy employ additional FPA cooling.

21. Selected Technology Presentations

Sofradir and CEA LETI review in paper -121 their work on how to reduce the power required by the Analog to Digital Converters (ADC) in cooled infrared focal plane arrays. The power consumption is a result of direct power consumption needed to supply the converter and indirectly, the power consumption needed to cool the increase of the chip size due to the ADC implementation. The result of this work is a fully digital ROIC with a power consumption in the same range as a fully analog circuit.

Prediction of system failures due to cooler malfunctioning is the subject of paper -122. In order to test the theoretical Weibull life distribution function, Ricor has conducted field reliability tests for one of their microcoolers. The results of this work are used in building preventive maintenance plans.

Agiltron demonstrates in paper – 123 their new chalcogenide glass lenses which have a thermal expansion coefficient close to that of aluminum and therefore form an athermal lens package when mounted in an aluminum housing. Furthermore, the material's temperature induced index of refraction is near zero and antireflective surfaces can be molded into the glass. This and the direct molding of lenses to net-shape without additional finishing operations are claimed to result in lenses of higher performance and lower cost.

Answering the need for higher resolution—see Fig. 32, SemiConductor Devices, SCD, presents in paper -124 the Hercules FPA which is their latest development of a new large format 2-D InSb detector with 1280 × 1024 elements and a pixel size of 15 μm. A new signal processor for use in this mega-pixel detector is described. The Readout Integrated Circuit (ROIC) is designed for, and manufactured with, 0.18 μm CMOS technology.

A new type of infrared filters, the Frequency Selective Surface (FSS), is demonstrated in paper -125 by Sandia National Laboratories and Sandia Staffing Alliance. The filters consist of a single layer of metal on a GaAs substrate. Their transmittance over a spectral and broad angular band, as well as their polarization response, may be tailored. Application in an FPA with individual pixels that are responsive to different spectral bands and polarizations is envisaged.

Fig. 32 From paper -124 showing imaging from a 1280 × 1024 InSb FPA with 15 µm pixels.

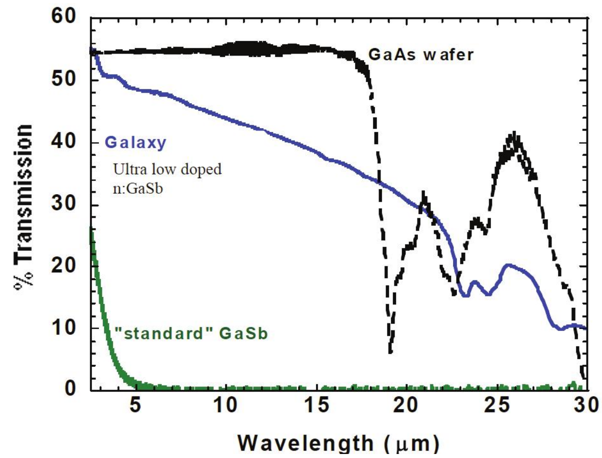

Fig. 34 Ultra-low-doped GaSb substrate material shows much higher transmission than standard GaSb —from paper -136.

L-3 Electro-Optical Systems analyzes in paper -126 what they term localized SNR, LSNR, from measured man and vehicle targets in the field. Image intensifier and uncooled LWIR cameras are used in the measurements. It is concluded that LSNR is greater for the fused dual sensor system mode than for a single system mode using the I2 or IR camera separately.

XenICs reports in paper -127 on their development of a high speed, QVGA format InGaAs camera with a frame rate as high as 1740 frames/sec and 120,000 single lines/sec. Hyperspectral imaging applications, which require frame rates that are a factor of 50 to 200 higher than for regular imaging applications, are considered suitable for this uncooled SWIR camera—see Fig. 33.

Galaxy Compound Semiconductors, AFRL, the University of Massachusetts, Lowell and Pacific Northwest National Laboratory discuss in paper -136 GaSb substrates which have advantages that make them attractive for implementation in a wide range of VLWIR detectors with higher operating temperatures for stealth and space based applications. Ultra low doped n:GaSb shows an improved transmission when compared to "standard" GaSb as shown in Fig. 34.

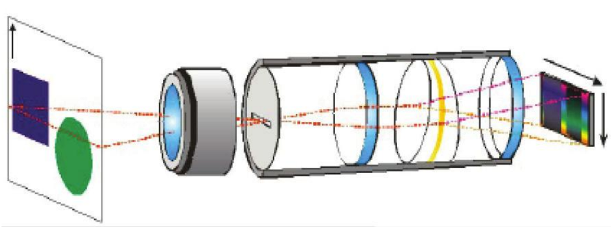

Fig. 33 Hyperspectral imaging spectrograph in which a line on the image is dispersed via a prism-grating-prism optical assembly and recorded by a SWIR camera—from paper -127.

22. Selected Application Presentations

Paper -129 by University of Victoria focuses on real-time assessment of wild-fire threats – a problem which cost the U.S. $ 10 billion in year 2000. The acquisition of fire characteristics by use of hyperspectral sensors, LIDAR, and multispectral thermal sensors together with sophisticated image processing is discussed and is illustrated in Fig. 35.

The importance of avoiding collisions between birds and aircraft during landing and take-off has been shown recently by the dramatic accident in New York's harbor. Paper -148 by Carl Zeiss reports on an early warning system against birds which consists of two thermal imagers operating in a stereoscopic mode. Warning times of several minutes are claimed for the system.

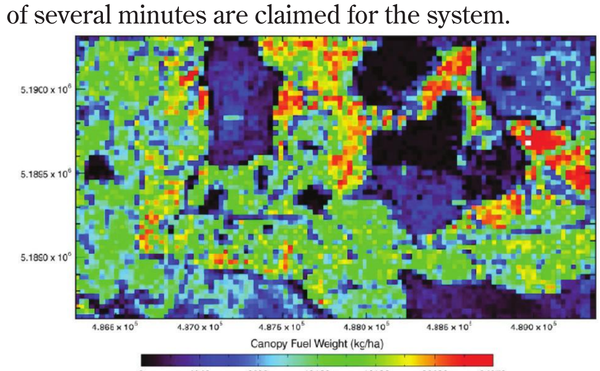

Fig. 35 Canopy fuel weight map, used to estimate fire behavior, is generated from sensors described in paper -129.

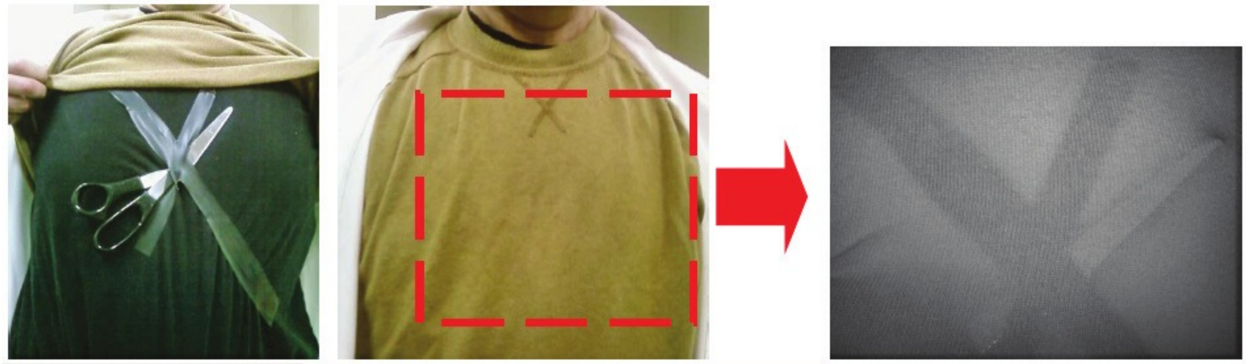

Fig. 36 Illustration of near-infrared detection of concealed objects under clothing—from paper -157.

Standoff detection of explosives and weapons concealed under clothing is the important security-related topic presented in G-Tronix' paper -157. A robust, portable, and low-cost NIR system is constructed from off-the-shelf components. The detections are made from a distance of 5 meters—see Fig. 36—while it is claimed that the distance may be extended to 50 meters without significant increase in cost and complexity.

A dual-camera dual-band system which measures temperature of and distance to radiometrically grey objects is outlined by Johns Hopkins University in paper -131. Multiple design approaches and trade-offs are described. Experimental data is analyzed and compared with model predictions. An explanation is suggested for the relatively large variation of 1 – 16% in temperature estimation error.

University of North Texas has designed, built and tested a tracking system using a programmable infrared beacon transmitter array, operating at 0.95 µm, and a micro-controller based receiver. The present version, described in paper -133, operates at a range of a few meters with signal bursts centered at a frequency of 38 kHz. It is claimed that the design may be extended to serve as an Identifier-Friend-Foe, IFF, in the battlefield. Theoretical and experimental investigation of the use of MWIR quantum cascade lasers, QCL, and absorption spectroscopy for standoff detection of TNT and TATP explosives at places like railway stations and airports are investigated by Fraunhofer Institut fur Physikaliche Messtechnik and reported in paper -137. The detection limits in the experimental set-up are found to be determined by the laser output noise and drift. External cavity QCL and multiple QCLs are considered for further improvement of system sensitivity. Figure 37 illustrates the system used.

The threat of liquid explosives has resulted in passengers being prohibited from travelling with bottles filled with liquids. Hydrogen peroxide is a typical component of these explosives. A team from Osaka University, paper -145, has developed an inspection system which determines the concentration of hydrogen peroxide in bottles by use of NIR absorption spectra and multivariate statistical analysis. The system—Fig. 38—having an inspection time of 5 seconds, will be installed at airports and will lead to a relaxation on the banning of bottles.

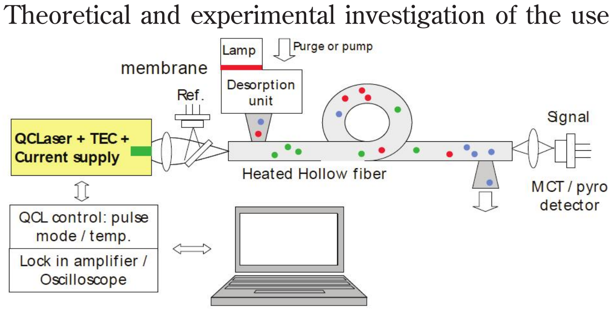

Fig. 37 Set up using quantum cascade laser for the detection of explosive materials as described in paper -137.

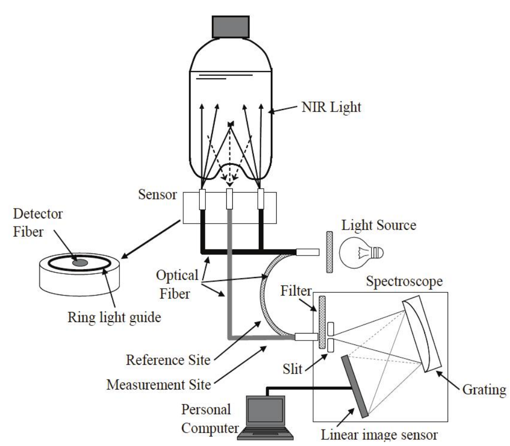

Fig. 38 Bottle inspection system for airport liquid inspection as reported in paper -145.

The National Institute of Standards and Technology, NIST, discusses in paper -150, their development of an advanced Absolute Cryogenic Radiometer, ACR, designed to enable the measurement and calibration of infrared power as low as 1 picoWatt with an accuracy on the order of 0.1 %. Experimental investigation reveals that the sensitivity of the new generation ACR will reach the expected increase by an order-of-magnitude above that of the existing version.

Paul R. Norton
Bjørn F. Andresen
Gabor F. Fulop